Electronic Phase Shifter for Millimeter-Wave Semiconductor Dielectric Integrated Circuits

HAROLD JACOBS AND METRO M. CHREPTA

Abstract—A new system is proposed for millimeter-wave integrated circuits. It is suggested that high-resistivity silicon be used as a medium for a dielectric waveguide. With the advent of high-resistivity silicon, propagation can occur with relatively low loss. Furthermore, since the medium is a semiconductor compatible with active devices, it is proposed that active devices can be constructed directly in the semiconductor dielectric guide or appendaged directly on the surface. The basic approach is similar to that used in integrated optics, except that the medium for millimeter-wave guidance is a semiconductor and the control devices rely on conductivity modulation rather than on electrooptical effects.

Some particular devices suggested are oscillators, mechanical and electronic phase shifters, amplitude modulators (switches), and detectors. The first of such devices investigated has been the electronic phase shifter. Related theory and experiments are reported here. In addition, preliminary results on oscillators imbedded in a dielectric resonator are presented.

I. INTRODUCTION AND BACKGROUND

IN THE APPROACH to millimeter-wave and submillimeter-wave circuitry, it has become apparent that the techniques commonly used in the microwave region are inapplicable. In the design of microwave integrated circuits using stripline, for instance, the losses are prohibitively high at frequencies higher than 30 GHz. In the case of waveguide components, operation can be obtained up to about 140 GHz and somewhat higher, but the cost of machining metal guides becomes increasingly a matter of concern. In addition, many of the active devices and components are really based on "lumped constant" principles and at higher frequencies the need exists for distributed devices and components, in order to become more compatible with the distributed parameters of the transmission line itself. It has therefore been proposed that from the region of 30 GHz up to 300 GHz and higher, optical techniques be employed.

One such approach used in the optical area is referred to as "integrated optics." In this approach [1]–[4], it was suggested that a waveguide made of glass could be used to transport electromagnetic radiation. Propagation is carried out in the E_{11}^{y} mode as indicated in Fig. 1, and modulating elements, couplers, etc., could be designed. Now the authors have proposed [5], [6] that a similar principle be applied to develop millimeter-wave integrated circuits. They have suggested the use of silicon (or gallium arsenide) dielectric waveguides to act as the transmission line. In addition, the devices and components often made of silicon could be "built in" the semiconductor line so that, in effect, one would have an optical line with active elements incorporated, all of which are compatible and all of which would serve to integrate millimeter-wave componentry.

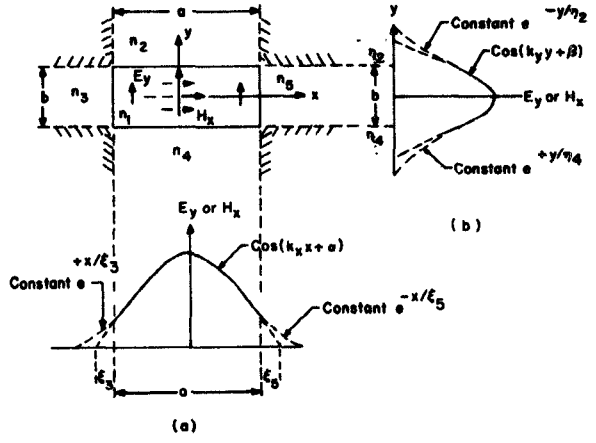

Fig. 1. Semiconductor guide immersed in air dielectric. (a) Cross section. (b) Field distribution of the fundamental E_{11}^{y} mode.

Some of the devices suggested for integration are listed as a source (IMPATT or Gunn generators), amplitude modulator or switch, directional couplers, phase shifters, and detector diodes. Some of these are sketched in Fig. 2.

With this background, we first considered an electronic

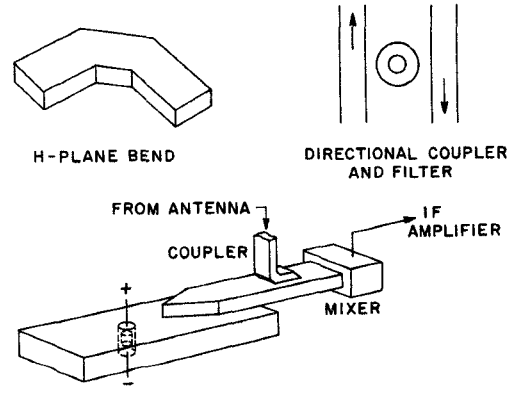

Fig. 2. Semiconductor dielectric waveguide devices and components.

Manuscript received June 22, 1973; revised October 17, 1973.

The authors are with the Semiconductor Devices and Integrated Electronics Technical Area, U. S. Army Electronics Technology and Devices Laboratory (ECOM), Fort Monmouth, N. J. 07703.

phase shifter. This device could be used as a tuner for impedance matching to a load, or for phase modulation, or for phased array scanning. Before describing the electronic phase shifter, however, we must first consider propagation in a semiconductor dielectric waveguide.

II. EQUATIONS FOR PROPAGATION IN DIELECTRIC WAVEGUIDE

The original theories derived by Marcatili [1] result in the following set of equations applied to Fig. 1. The propagation constant in material ν is

$$k_\nu = kn_\nu = \frac{2\pi}{\lambda} n_\nu. \tag{1}$$

In the semiconductor waveguide, we understand $k_\nu = k_1$ so that

$$k_z^2 = (k_1^2 - k_x^2 - k_y^2). \tag{2}$$

Also,

$$k_x = k_{x1} = k_{x2} = k_{x4} \tag{3}$$

$$k_y = k_{y1} = k_{y3} = k_{y5}. \tag{4}$$

The attenuation constants are

$$k_{y2} = -\frac{1}{\eta_2}, \quad k_{x3} = -\frac{1}{\xi_3}. \tag{5}$$
$$\underset{4}{} \qquad\qquad \underset{5}{}$$

The propagation constant vector components are given by

$$k_x = \frac{p\pi}{a}\left(1 + \frac{A_3 + A_5}{\pi a}\right)^{-1} \tag{6}$$

$$k_y = \frac{q\pi}{b}\left(1 + \frac{n_2^2 A_2 + n_4^2 A_4}{\pi n_1^2 b}\right)^{-1} \tag{7}$$

$$k_z = \left[k_1^2 - \left(\frac{\pi p}{a}\right)^2\left(1 + \frac{A_3 + A_5}{\pi a}\right)^{-2} - \left(\frac{\pi q}{b}\right)^2\left(1 + \frac{n_2^2 A_2 + n_4^2 A_4}{\pi n_1^2 b}\right)^{-2}\right]^{1/2} \tag{8}$$

Here,

$$A_{2,3,4,5} = \frac{\pi}{(k_1^2 + k_{2,3,4,5}^2)^{1/2}} = \frac{\lambda}{2(n_1^2 - n_{2,3,4,5}^2)^{1/2}} \tag{9}$$

and

$$\xi_3 = \frac{1}{|k_{x3}|} = \frac{1}{[(\pi/A_3)^2 - k_x^2]^{1/2}} \tag{10}$$
$$\underset{5}{} \qquad \underset{5}{}$$

$$\eta_2 = \frac{1}{|k_{y2}|} = \frac{1}{[(\pi/A_2)^2 - k_y^2]^{1/2}} \tag{11}$$
$$\underset{4}{} \qquad \underset{4}{}$$

and it is assumed that

$$[k_x A_3/\pi]^2 \ll 1 \quad \text{and} \quad [k_y A_2/\pi]^2 \ll 1. \tag{12}$$
$$\underset{5}{} \qquad\qquad \underset{4}{}$$

Furthermore, a is the x dimension, and b is the y dimension of the guide.

In applying these equations to high-resistivity silicon surrounded by air, we assume the dielectric constant of silicon ϵ_R is 12. That is, $n_1 = 12$ for silicon and $n_2 = n_3 = n_4 = n_5 = 1$ for air. With this background, we can now describe several experiments related to propagation in the semiconductor.

III. MEASUREMENT TECHNIQUES

Long lengths of semiconductor (resistivities greater than 10 000 Ω·cm silicon) dielectric waveguide were prepared with different cross-sectional geometries. We refer to these as cases 1, 2, and 3. In case 1, the dimensions were $a = 1.58$ cm, $b = 0.79$ cm. In case 2, $a = 1.58$ cm, $b = 0.3$ cm. In case 3, $a = 0.5$ cm and $b = 0.3$ cm. In these experiments, the frequency was maintained at 16.4 GHz. In later experiments, the frequency was set at 70.5 GHz, and here, the samples were $a = 0.31$ cm and $b = 0.155$ cm in cross-sectional dimension. The first tests were run at *Ku* band only because of ease of fabrication and availability of electrical equipment.

In case 1, the wavelength in the material is

$$\lambda_1 = \frac{c}{f}\frac{1}{(12)^{1/2}} = \frac{3 \times 10^{10}}{1.64 \times 10^{10}}\frac{1}{3.46} = 0.53 \text{ cm}$$

so that the dielectric waveguide can be considered to be oversized in both the a and b dimensions; in case 2, only in the b dimension; and in case 3 we did not have the oversized waveguide. In the method of measurement for all three cases, the ends were tapered for transitions with minimal reflection from a standard *Ku*-band waveguide operating in a TE_{10} mode to dielectric waveguide. Where the b dimension of the dielectric was considerably smaller than 0.79 cm of the conventional waveguide, metal transitions were placed on top and bottom inside the waveguide as shown in Fig. 3. Now, λ_z was measured in several possible arrangements. In Fig. 4, a probe was placed just above the silicon surface, and VSWR-type measurements were made. To measure λ_z in the arrangement of Fig. 5, we used a metal waveguide filled with silicon dielectric and placed it in the test section. Here, we calculated λ_{zg} the guide wavelength, with a silicon-filled waveguide. Next, the piece was taken out and the metal waveguide cover removed. The silicon alone was then inserted in the test section and the phase change noted. Then, using

$$\Delta\phi = \phi_z - \phi_{zg} = \left(\frac{2\pi}{\lambda_{zg}} - \frac{2\pi}{\lambda_z}\right)\Delta l \tag{13}$$

where Δl is the length of semiconductor, λ_{zg} is the wavelength in the silicon-filled metal waveguide, and λ_z is the wavelength in the silicon dielectric waveguide, we could determine $\Delta\phi$. Checks of this sort (replacement techniques) have been run with oversized waveguides and gave almost perfect agreement with theory.

Another method of using the setup in Fig. 5 was also tried which gave more flexibility. The test section con-

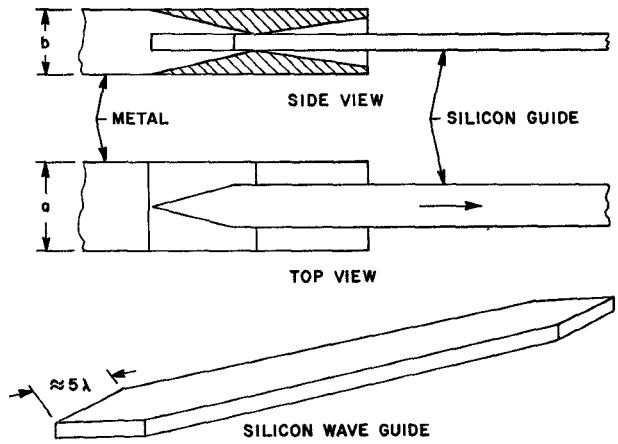

Fig. 3. Launcher from metal waveguide to dielectric waveguide.

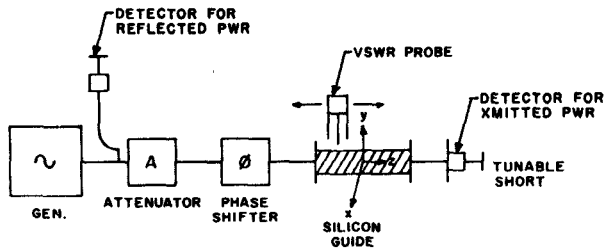

Fig. 4. Arrangement for λ_z measurement.

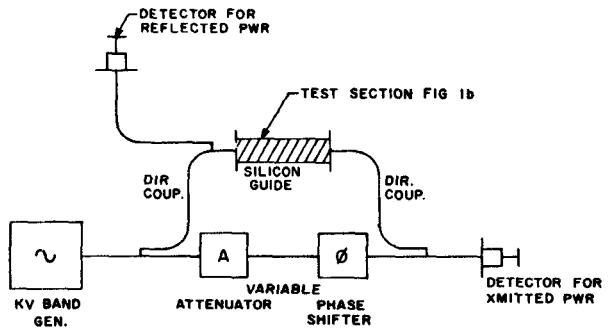

Fig. 5. Experimental setup to measure λ_z, λ_{zg}, α, ϕ.

sisted of a silicon dielectric waveguide with transition points and no metal covering. Here the wavelength λ_z could be calculated. Next, a metal plate was placed on top of the silicon, and λ_z' the wavelength with metal cover, was calculated. Then, by (13), the calculated phase shift was compared with the experimental phase shift measured with the bridge. The physical arrangement is shown in Fig. 6 for the insertion of the semiconductor in the test section and covering the upper surface with a conducting medium.

IV. MECHANICAL PHASE SHIFTING IN DIELECTRIC WAVEGUIDES

We shall now describe experiments in which measurements were made on changes in phase shift due to the presence of a metal plate placed on top of the upper boundary.

In carrying out the calculations relating to these experiments, we shall use the equations produced by Marcatili [1] rather than nomographs, charts, etc. The reason for this is that we want to get deeper insight into the behavior of the propagation constants in order to appreciate the mechanisms of their changes. In addition, in comparing theory and experiment, one can better appreciate the reasons for differences.

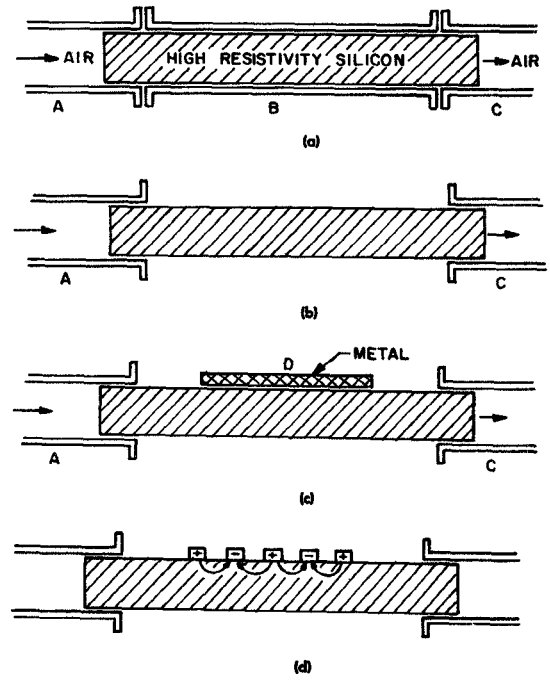

Fig. 6. Waveguide test section.

Case 1: Here,

$$f = 16.4 \text{ GHz} \qquad a = 1.58 \times 10^{-2} \text{ m} \qquad n_{2,3,4,5} = 1$$

$$\lambda_{air} = 1.83 \times 10^{-2} \text{ m} \qquad b = 0.79 \times 10^{-2} \text{ m}$$

$$n_1 = 3.464 \qquad p = q = 1$$

and

$$A_j = \frac{\lambda_{air}}{2(n_1^2 - n_j^2)^{1/2}} = 2.76 \times 10^{-3}, \qquad j = 2,3,4,5$$

$$k_x = \frac{p\pi}{2}\left(1 + \frac{A_3 + A_5}{\pi a}\right)^{-1} = 179$$

$$k_y = \frac{q\pi}{b}\left(1 + \frac{n_2^2 A_2 + n_4^2 A_4}{\pi n_1^2 b}\right)^{-1} = 392$$

$$k_1 = \frac{2\pi n_1}{\lambda_{air}} = 1186$$

$$k_z = [k_1^2 - k_x^2 - k_y^2]^{1/2} = 1105$$

$$\lambda_z = \frac{2\pi}{k_z} = 5.68 \times 10^{-3} \text{ m} \qquad (14)$$

where k_z and λ_z refer to the propagation constant and wavelength in the direction of propagation for the E_{11}^y mode for the silicon dielectric waveguide (Fig. 7).

With the metal on top, k_y' behaves approximately as if the height b were doubled [7], and the propagation vector

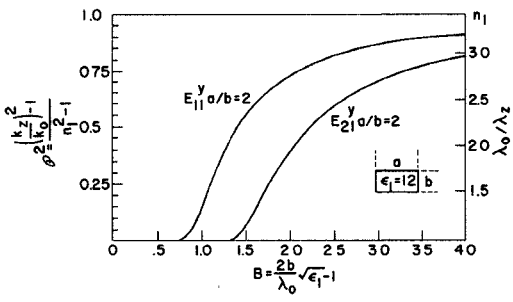

Fig. 7. Propagation constants as a function of dimensions of dielectric waveguide.

components change as follows:

$$k_x' \text{ remains the same} = 179$$

$$k_y' = 195$$

$$k_z' = 1160$$

$$\lambda_z' = 5.43 \times 10^{-3}\,\text{m} \qquad (15)$$

where the primes indicate the semiconductor is covered with a metal top. The change in λ_z can be determined from the value of b in Fig. 7.

The calculated phase shift from 1 cm of metal cover to no metal is

$$\Delta\phi = (k_z' - k_z)\Delta l = (1160 - 1105)10^{-2} \cong 33°. \qquad (16)$$

By experiment in four runs, we obtained a value of 35°/cm which indicates that the agreement between theory and experiment is good for the oversized waveguide (case 1). Further details are shown in Table I.

Next, we consider case 2, where $a = 1.55 \times 10^{-2}$ m and $b = 0.3 \times 10^{-2}$ m and case 3 where $a = 0.5$ cm and $b = 0.3$ cm. Using (14) again with $f = 16.4$ GHz, $\lambda_{air} = 1.83 \times 10^{-2}$, calculations were made of the propagation constants of the silicon dielectric waveguide with no metal on the upper surface and then with a metal plate applied to the upper surface.

In Table II, we have listed the results of calculations and experiments related to mechanical phase shifting. Several conclusions become apparent. In applying the "integrated optics theory" to silicon waveguide, agreement is better on slightly oversized waveguides. Smaller dimension waveguides give only approximate agreement. This is because with smaller dimensions the k_x and k_y terms become large and approximations pertaining to "nearly" TE modes start to become invalid. Even with some apparent disagreement in the case of smaller cross-section waveguides, the approximation technique of Marcatili is still exceedingly useful in that it gives good physical insight and meaning into how the waves are actually behaving in and around the semiconductor. For this reason, when combined with some direct measurements, the Marcatili approximations perform a vital service.

We also note that a mechanical phase shifter in itself could be a useful device. In no case did we find any perceptible change in attenuation with change in phase, and in addition, the insertion loss was nearly zero.

TABLE I
PHASE SHIFT—MEASURED VERSUS CALCULATED[a]

Length of Metal l(cm)	Phase Shift $\Delta\phi$ Measured (degrees)	Phase Shift $\Delta\phi$ Calculated (degrees)
0.6	20	22
1.9	62	70
3.8	100	141
8.0	272	300

[a] In all of these experimental changes in phase shift, there was no observable change in the attenuator (A) required to find the null point of the bridge.

TABLE II
COMPARISON OF CALCULATED AND EXPERIMENTAL VALUES OF PHASE SHIFT PER CENTIMETER WITH AND WITHOUT METAL PLATE ON UPPER SURFACE

	CASE NO. 1	CASE NO. 2	CASE NO. 3
	b = 0.79 cm	b = 0.3 cm	b = 0.3 cm
Marcatili Approximation	a = 1.58 cm	a = 1.55 cm	a = 0.5 cm
A_j	2.76×10^{-2} m	2.76×10^{-3} m	2.76×10^{-3} m
k_x	179 m^{-1}	177 m^{-1}	462 m^{-1}
k_y	392 m^{-1}	998 m^{-1}	998 m^{-1}
k_z	1105 m^{-1}	638 m^{-1}	457 m^{-1}
k_1	1186 m^{-1}	1186 m^{-1}	1186 m^{-1}
λ_z	5.68×10^{-3} m	9.85×10^{-3} m	1.375×10^{-2} m
With Metal On Top Surface			
k_x'	179 m^{-1}	177 m^{-1}	426 m^{-1}
k_y'	195	525	525
k_z'	1160	1060	955
λ_z'	5.40×10^{-3} m	5.92×10^{-3} m	6.55×10^{-3} m
Calculated Change in Phase Angle Metal On Top Surface Vs. No Metal			
$\Delta\phi$/cm	33°/cm	192°/cm	300°/cm
Measured $\Delta\phi$/cm	32°/cm	161°/cm	250°/cm

A more general way of looking at the action in changing λ_z and phase angle is obtained by considering normalized graphical techniques. Using Marcatili's and Goell's normalized propagation constant $P^2 = [(k_z/k_0)^2 - 1]/[n_1^2 - 1]$ and normalized guide height $B = (2b/\lambda_0)(n_1^2 - 1)^{1/2}$ to plot the propagation curves for the fundamental E_{11}^y and E_{21}^y modes, it is convenient for observing the percentage of energy contained within the guide for various waveguide dimensions, aspect ratios, and refractive indices. Also, Knox and Toulios [9] plotted λ_0/λ_z versus B which varies from 1 to n_1 as a function of the normalized height of the guide. This plot shows the poor guidability at $\lambda_0/\lambda_z = 1$, where almost all of the energy is external to the guide. At $\lambda_z = n_1\lambda_0$ for a wide range of B, the energy, is almost wholly contained within the guide.

Placing the metal boundary on the waveguide effectively doubles the height or B dimension obtaining the image guide configuration as reported by Knox, Toulios, Schlesinger, and King. For example, in the E_{11}^y curve depicted in Fig. 7, a change in B from 1 to 2 shows a λ_0/λ_z change from 1.4 to 2.8, a decrease in λ_z. The assumption is made here that the change in results is small even with a change in ratio of a/b or the aspect ratio. This approach shows in one glance why the wavelength

(and hence, phase) changes in the dielectric waveguide when one covers the dielectric with metal and, hence, changes its b dimension.

V. ELECTRONIC PHASE SHIFTING

The mechanical phase shifter leads to another possibility. Suppose instead of applying a metal to the upper surface of the semiconductor we attach a semiconductor plate to the upper surface. This plate might have built-in p-i-n structures so that it becomes conducting or nonconducting. This would be equivalent to mechanically placing a metal plate on the surface or removing it. Some suggested structures are shown in Fig. 8.

All of these structures have been tried and best results have been obtained with arrangements in Fig. 8(b) and (c). We shall next describe the experiment in greater detail.

First, for the test section of the silicon dielectric waveguide, a piece was cut, ground, and polished to the dimensions of 0.3 by 0.5 cm. This was used in the greatest number of experiments.

The silicon waveguide was inserted in the test section of the bridge shown in Fig. 5. The net insertion loss for the dielectric guide only was about 1 dB due to mismatch at the launch ends. This gives a transition loss at each end of 0.5 dB per transition.

The first type of electronic phase modulator was constructed as follows. Junctions were formed in a silicon piece with initial resistivity of 10 000 Ω·cm. The geometry is shown in Fig. 9. This p-i-n diode was then placed on the upper surface of the silicon guide, 0.5 × 0.3 cm in dimension. With this particular sample, when the modulator was placed on the silicon guide, there was a 6-dB mismatch with the arrangement shown in Fig. 10. But, beyond this, there was no change in attenuation with forward bias of the p-i-n diode. Experimental results are shown in Fig. 10.

At optimum phase shift conditions, we obtained $\Delta\phi = 26°$ or, for an active length of junction region of 0.45 cm, the phase shift was 58°/cm. The insertion loss was about 5.9 dB, but most of this was due to excess metallization for contact to the junction regions. From tests on other samples, the insertion loss due to mismatch of the diode with this geometry was about 2 dB.

Next, we consider another experimental sample 6. Here, the geometry was the same as indicated in Fig. 9. The specimen was originally 3 mm in height with the junction region as indicated. The bottom edge was ground and polished so that the junction region of the appendage was closer to the silicon waveguide, 0.3 × 0.5 cm in cross section. This resulted in moving the junction regions down closer to the waveguide. The insertion loss was 3 dB at 16.4 GHz and little or no change in attenuation was noted during the phase shifting process. The active region of the junction was 0.6 cm in length so that the phase shift per centimeter was 30°/0.6 cm = 50°/cm.

In the next run, the same sample 6 was heavily coated

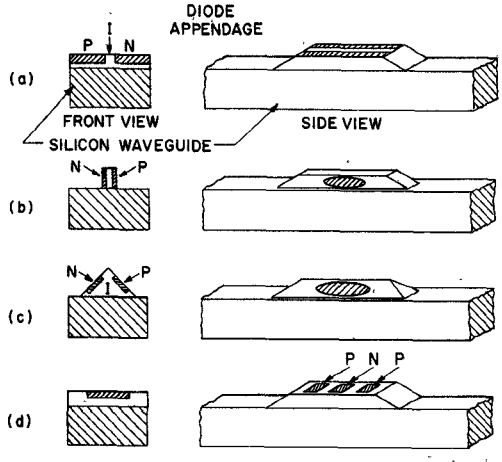

Fig. 8. Geometries of electronic phase modulator.

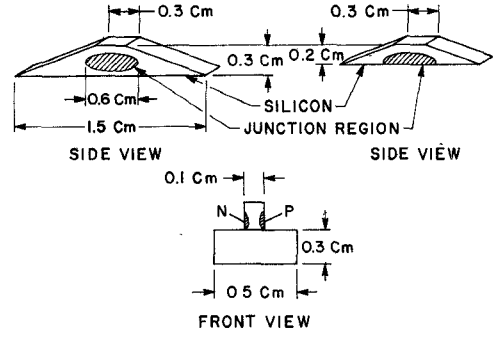

Fig. 9. Electronic phase shifter.

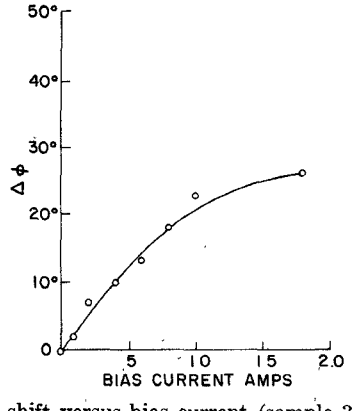

Fig. 10. Phase shift versus bias current (sample 3, 0.45-cm active length).

with indium in order to make better contact to the metallized junction regions. The metallization of the junctions is now Cr coating, CrAu coating, Au coating, and In coating (heavy as in a solder contact). Here the insertion loss was 3 dB due to mismatch. Also, unlike the previous samples, the presence of large In contacts seemed to reflect more loss into the line during phase shifting, but the phase shift was enhanced. Now 58°/0.6 cm of active region was found or 97°/cm. Data are indicated in Fig. 11.

Experiments were also tried at 70.5 GHz using the bridge techniques as shown in Fig. 5. Here the inner dimensions of the metal guide were 0.366 × 0.183 cm and

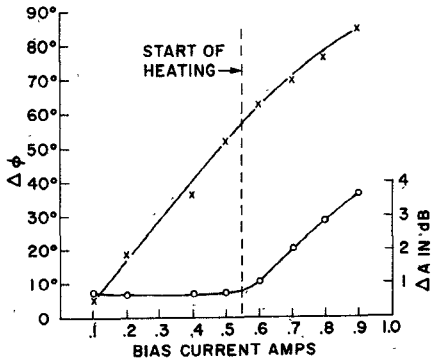

Fig. 11. Phase shift versus bias current (Sample 6, In coated).

the semiconductor dielectric waveguide was 0.314 × 0.157 cm. Thus the silicon guide was oversized. A rough estimate of λ_z and $\Delta\phi/\Delta l$ for the $E_{11}{}^y$ mode can be obtained as follows. From direct calculation or from Fig. 7 with B = 2.7, $\lambda_z = \lambda_0/3.15 = 0.426/3.15 = 0.135$ cm. Then $k_z = 2\pi/0.135 = 46.50$ cm^{-1}. With the metal image plane, $B = 5.4$.

We estimate that this gives a λ_z close to that found in the infinite semiconductor medium and $\lambda_z \cong \lambda_0/n_1 = 0.426/(12)^{1/2} = 0.123$ cm and $k_z' = 6.28/0.123 = 51.0$ cm^{-1}. With $\Delta\phi/\text{cm} = (51.0 - 46.5) = 4.5$ rad, we obtain 255°/cm.

Now in measurements with a metal strip, we obtain data as in Table III. Here again, for the case of a slightly oversized waveguide, the agreement of calculated wavelength λ_z in the semiconductor waveguide with measured values is good. We have also assumed in this calculation that the transition from the TE_{10} mode in the metal waveguide to the $E_{11}{}^y$ mode in the silicon guide is made with little probability of a jump to higher $E_{mn}{}^y$ modes. This assumption appears to have worked well.

Next, we describe an electronic phase shifter operating at 70.5 GHz. The p-i-n diode now consisted of a silicon piece approximately 1 cm in length. Its cross section was triangular in shape, as shown in Fig. 8(c) and Fig. 12. Each edge was approximately 0.3 cm so that when the p-i-n diode was placed on the waveguide surface, almost all of the area of the guide under the diode was covered. As in the case of the other diodes previously described, the junctions were formed by metal arcing in a Forming Gas atmosphere.

In this case, as excess carriers are injected in the forward bias condition, the high conductivity starts at the uppermost edge of the triangular piece. As current is increased, the conductivity increases in a downward motion. This is essentially controlling the height of the dielectric guide. Thus in changing the effective b dimension k_y decreases, increasing k_z for a change in λ_z. Experimental results are shown in Fig. 13. There was no change in attenuation with bias current up to 1.75 A. At this point, there was a 35° change in phase. The initial mismatch loss due to placing the modulator on the silicon semiconductor guide was less than 2 dB. The increase in attenuation shown was caused by heat transfer from the diode to the guide.

TABLE III
MEASURED CHANGES IN PHASE SHIFT WITH METAL PLATE

Length of Metal (centimeters)	Measured $\Delta\phi$ (degrees)	Calculated $\Delta\phi$ (degrees)
0.2	45	51
0.5	130	130
0.8	206	204
1.0	247	255

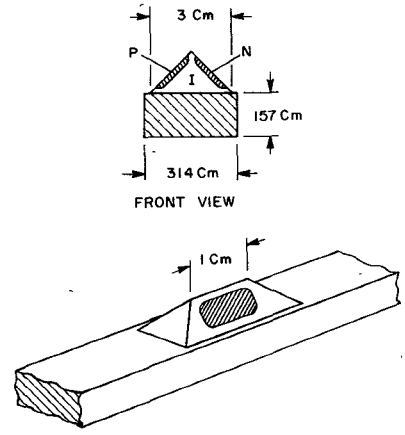

Fig. 12. 70-GHz phase shifter.

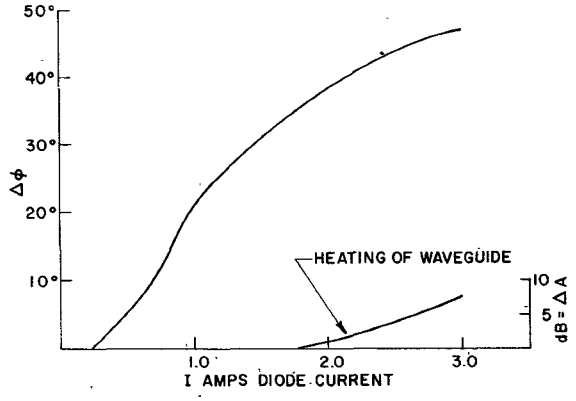

Fig. 13. Phase shift versus bias current (70.5 GHz).

VI. SILICON SLAB OSCILLATOR

Utilizing the characteristics of a wave in a high dielectric medium, a resonant structure was fabricated as shown in Fig. 14. A Gunn or IMPATT diode was mounted on a post in the center of a silicon slab. The resonant frequency is dependent upon the number of half wavelengths on each side of the diode. The energy was coupled as shown into a silicon waveguide system where the frequency and the power were monitored. The guide wavelength or tuning can be accomplished by placing the diode used in the phase shifter experiments onto the coupled waveguide. In this manner, the B normalized height of the slab resonator is electronically controlled as in the phase shifter by modulating the conductivity over the coupling length, varying the resonant dimensions of the slab of silicon.

Using an X-band Gunn diode mounted in the silicon

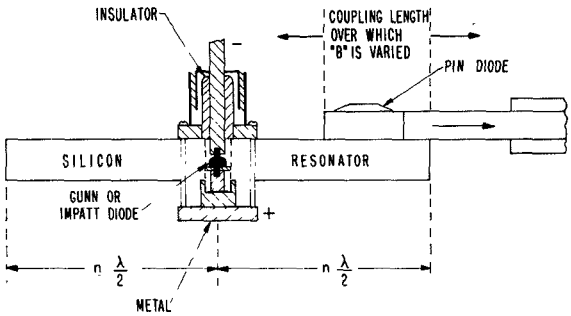

Fig. 14. Ku-band oscillator in silicon dielectric cavity.

slab at approximately one-third of the optimum rate input power (4.5 V, 0.500 A), the diode oscillated at 14.8 GHz with 20 mW output. The preliminary experimental results with this configuration showed greater than 200-MHz tuning range with the maximum current injection into the phase modulating p-i-n diode. The output power over this frequency tuning range varied only slightly. This experiment demonstrates that an oscillator can be constructed with a silicon dielectric waveguide, and in addition, resonant wavelength can be changed with the electronic modulator previously described. A disk resonator was also designed and constructed using an image plane that also served as a heat sink for the diode. Preliminary results are encouraging.

VII. CONCLUSION

An approach to millimeter-wave integrated circuits has been suggested in which silicon dielectric waveguides are used as a transmission line. Compatible devices and components can be built into the line or attached to the line in such a manner that generation, control, and processing of the signal can be carried out by conductivity modulation techniques. Experiments have been carried out illustrating the characteristics of mechanical and electronic phase shifters. In addition, preliminary work on an oscillator imbedded in a dielectric cavity has been demonstrated.

The results presented here do not represent optimum performance. The geometry of the phase shifters should be optimized for minimum dimensions and minimum loss. The silicon oscillators are multiwavelengths long. The performance could be improved with shorter slabs and optimized impedance posts.

REFERENCES

[1] E. A. J. Marcatili, "Dielectric rectangular waveguide and directional couplers for integrated optics," *Bell Syst. Tech. J.*, vol. 48, pp. 2071–2102, Sept. 1969.
[2] S. E. Miller, "Integrated optics: An introduction," *Bell Syst. Tech. J.*, vol. 48, pp. 2059–2070, Sept. 1969.
[3] D. Marcuse, *Light Transmission Optics*. New York: Van Nostrand-Reinhold, 1972.
[4] W. Schlosser and H. G. Unger, "Partially filled waveguides and surface waveguides of rectangular cross section," in *Advances in Microwaves*, vol. 1, L. Young, Ed. New York: Academic, 1966.
[5] M. M. Chrepta and H. Jacobs, "Bulk semiconductor quasi-optical concept for guided waves for advanced millimeter wave devices," Fort Monmouth, N. J., Tech. Rep. ECOM-3482, Sept. 1971.
[6] ——, "A bulk semiconductor millimeter wave phase shifter," Fort Monmouth, N. J., Tech. Rep. ECOM-3513, Nov. 1971.
[7] S. P. Schlesinger and D. D. King, "Dielectric image lines," *IRE Trans. Microwave Theory Tech.*, vol. MTT-6, pp. 291–299, July 1958.
[8] E. C. Jordan and K. G. Balmain, *Electromagnetic Waves and Radiating Systems*. Englewood Cliffs, N. J.: Prentice-Hall, 1968, pp. 273–275.
[9] R. M. Knox and P. P. Toulis, "Integrated circuits for the millimeter through optical frequency range," in *Proc. Symp. Submillimeter Waves*, vol. XX, Apr. 1970, pp. 497–515.